Electronic Supplementary Material (ESI) for Chemical Communications

Electronic Supplementary Information for

An Integrated AFM-Raman Instrument for Studying Heterogeneous Catalytic Systems: A First Showcase

Clare E. Harvey, Evelien M. van Schrojenstein Lantman, Arjan J. G. Mank and Bert M. Weckhuysen

A. Detailed information of the AFM-Raman setup

The integrated AFM-Raman setup consists of a Renishaw InVia micro-spectrometer coupled to an NT-MDT NTEGRA Spectra atomic force microscope (AFM). The combination was based on the creation of an extra laser path through the InVia that leads out of the system and into the NTEGRA Spectra.

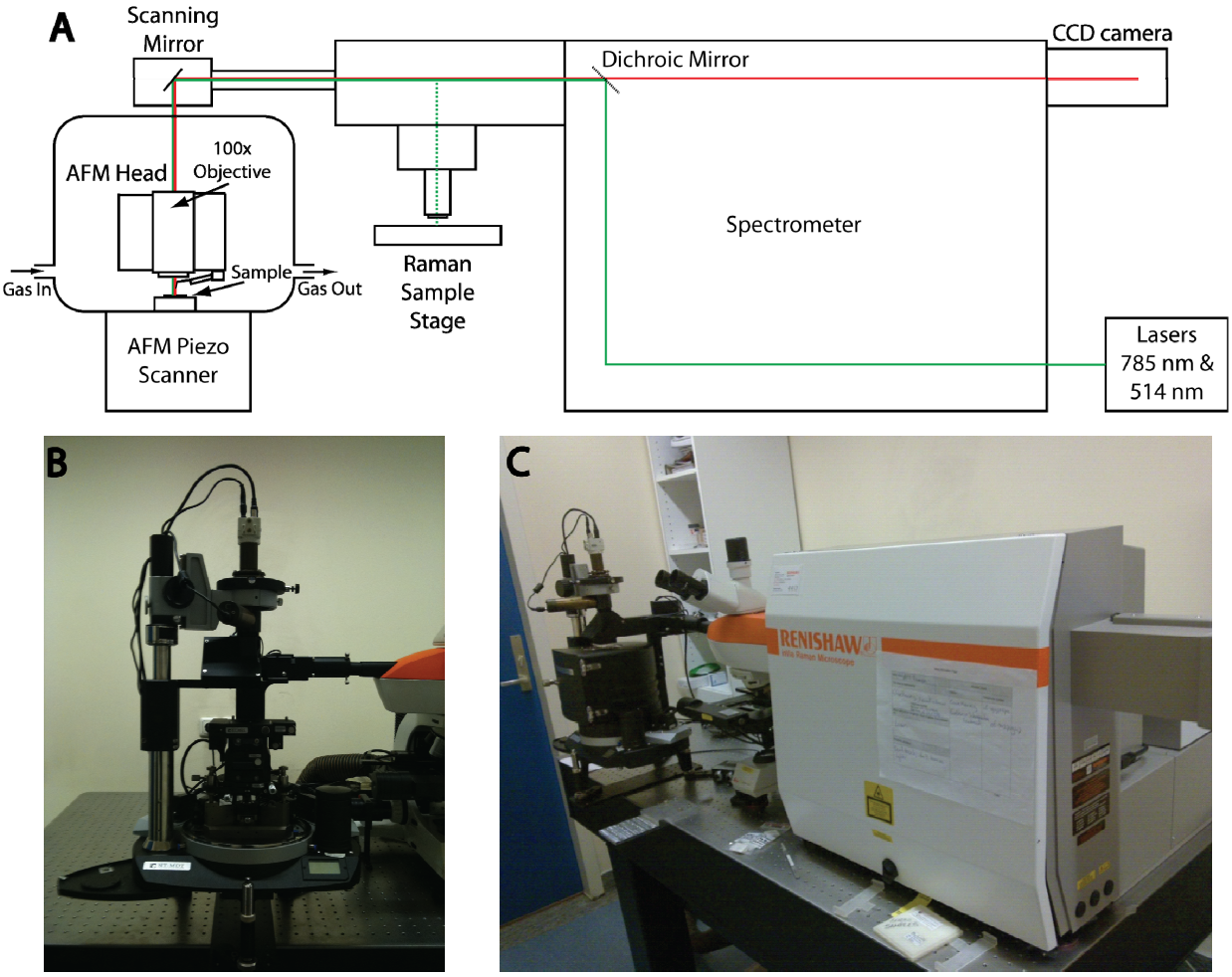

***Figure S1**:* A) Set-up schematic and light path from lasers, through Renishaw InVia to NT-MDT NTEGRA Spectra and back to Renishaw RenCam CCD camera; B) photograph of the NTEGRA AFM head and laser coupling, and C) photograph of the integrated AFM-Raman setup with the in-situ chamber around the AFM head.

B. Experimental Section

Silver nanoparticles were synthesized using methods documented by Lee and Meisel, Sun and Xia, and Cathcart.[27-29] Ag nanocubes synthesized using the Xia method have a maximum concentration of 25 nMol.L^{-1}. Rhodamine-6G (Rh6G) aqueous solution was prepared from the solid dye (Sigma Aldrich, purity ~ 95%) using MilliQ Type II ultrapure water (18.2 MΩ.cm^{-1}). α-Al_2O_3 wafers were sourced from Surface Preparation Laboratories ((001) surface, with a typical flatness of < 0.5 nm). Sample preparation was carried out by drop-casting 10 µL Ag nanoparticles on the polished Al_2O_3 wafer, then drop-casting 10 µL Rh6G solution over the dried Ag nanoparticles.

The set-up is based on an NT-MDT NTEGRA Spectra upright AFM unit integrated with a Renishaw InVia Raman microscope. A 100x 0.6 NA Mitutoyo objective, a 633 nm laser and a 785 nm laser were used for measurements in air, a 785 nm laser was used for all measurements in N_2. Olympus AC 160TS 'elephant trunk' tips were used for all AFM and AFM-Raman measurements. N_2 atmosphere measurements were carried out with an NT-MDT acoustic isolation chamber enclosing the AFM setup. Heating studies were carried out using an NT-MDT AFM heating stage (SU045NTF) placed on top of the AFM sample stage. High resolution AFM height images were all measured with 512 points in x and y directions. Combined AFM-Raman integrated measurements were all carried out with 64 points in x and y direction.

C. Influence of Ag nanoparticle morphology on SERS enhancement

For SERS the most commonly used way to produce Ag nanoparticles is the Lee and Meisel synthesis, [28] where the aggregation of the spherical nanoparticles results in a highly SERS enhancing substrate. However in this study we are interested in low surface densities of nanoparticles, up to single nanoparticle level, as this is most relevant for catalytic studies. Different Ag nanoparticles morphologies were tested to identify the form of nanoparticles that gave the highest SERS enhancement of Rh6G. Samples were prepared by drop casting the Ag nanoparticles solutions onto a polished Al_2O_3 wafer, followed by a drop of 10 µM Rh6G solution. For each sample a map of 64 × 64 Raman spectra was measured, with the intensity distribution shown in Figure S2.

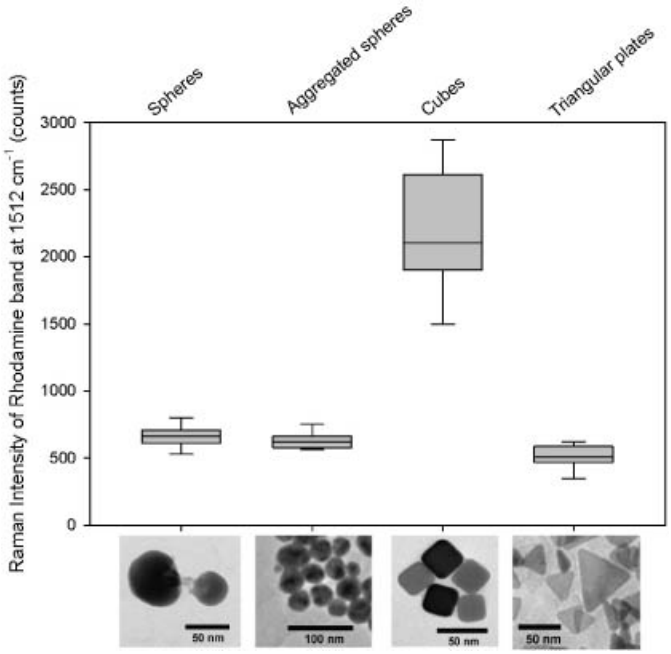

Figure S2: SERS enhancement of Rh6G for different Ag nano-particle morphologies. Measurements were carried out with a Renishaw InVia microscope using a 785 nm laser, 1 s exposure time, and a Leica 100x 0.85 NA objective.

The comparison of different Ag nanocrystal morphologies shows that nanocubes clearly induce a much higher SERS enhancement than spherical, aggregated spherical or triangular nanoparticles, which makes them well suited for working at low analyte concentrations. Nanoparticles with sharp edges give a higher SERS enhancement due to the nature of nanoparticle surface

plasmons, which are known to be one of the main factors in SERS enhancement. It is surprising that the planar triangular Ag nanoparticles did not also give a higher SERS enhancement, but this could be due to the character of the surface plasmons that causes the enhancement to be restricted by the planar nature of the nanoparticles.

D. Integrated AFM-Raman measurements in Air and N_2

Samples for combined AFM-Raman measurements were prepared using the same drop casting method as previously mentioned. Measurements are typically composed of a high resolution 20 x 20 µm AFM measurement of the surface (typically 512 x 512 points) followed by a combined AFM-Raman image of the same area, using 64 x 64 measurements points across each row. The Rh6G intensity images are made by mapping the intensity of the peak at 1512 cm^{-1}, the highest intensity peak in the spectrum that does not overlap with Raman bands originating from the Al_2O_3 substrate. The entire mapped area is measured repeatedly to measure photochemical behaviour for different Ag cluster sizes. The time-period for which measurement of such a surface was found to be possible without have to make system adjustments was in the order of 24 h. This means that even slow changes on the particles can be followed without any problem.

Figure S3 shows the AFM-Raman measurements for a sample measured in N_2. A high concentration of Ag nanocubes is evident from the AFM image.

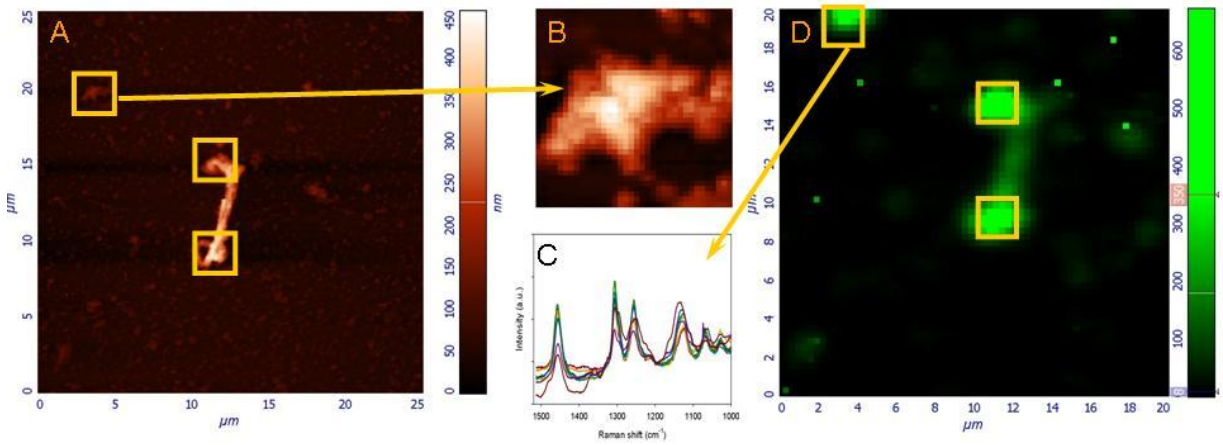

Figure S3: Simultaneous AFM and Raman imaging of an Al_2O_3 wafer coated with Ag nano-cubes and Rh6G in N_2 using a 785 nm laser, laser power 160 mW at sample; (A) AFM height image of surface; (B) AFM magnification of an area over which Raman intensity was followed (scale bar = 400 nm); (C) Raman spectra followed over time from area B; (D) Raman intensity map of the Rh6G band at 1512 cm^{-1}.

Combined AFM-Raman experiments in air and in a N_2-atmosphere were performed, to both confirm that the degradation of Rh6G is indeed due to a photo-reaction with air and to simultaneously test the setup for catalytic studies under non-ambient gas environments. For this purpose, an in-situ chamber was positioned over the AFM head. Despite higher noise levels, a small initial decrease in the Rh6G SERS spectrum was observed, followed by only a slight reduction in peak intensity in time (Fig. S4). It is likely that the initial signal intensity reduction is due to the reaction of Rh6G with residual O_2 on the sample surface. At long laser exposure times a change in the SERS spectrum of Rh6G was observed, with a new peak appearing at 1420 cm^{-1}. This indicates that there is another process occurring, the products of which must still be present at the SERS hotspot or they would not be visible at the low concentration level used.

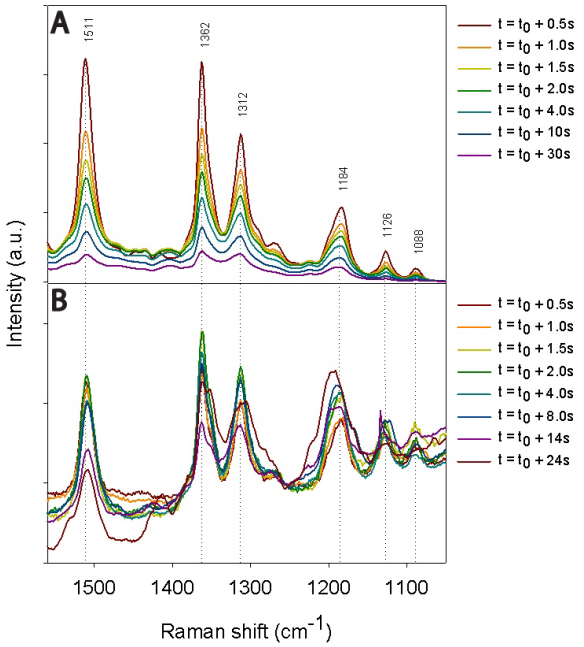

Figure S4: Comparison of the photo-degradation of Rh6G in air and in N_2 using a 785 nm laser (laser power 1 mW at sample) for Al_2O_3-supported Ag nanocubes.

Combined AFM-Raman measurements of the Al_2O_3-supported Ag nanocubes with Rh6G were carried out with both a 633 nm and 785 nm laser. Figure S5 shows a direct comparison of the Raman spectra of Rh6G recorded over time with both wavelengths. When plotting the intensity decrease of the Rh6G peak at 1512 cm^{-1} it can be seen that at both wavelengths the signal intensity decreases dramatically.

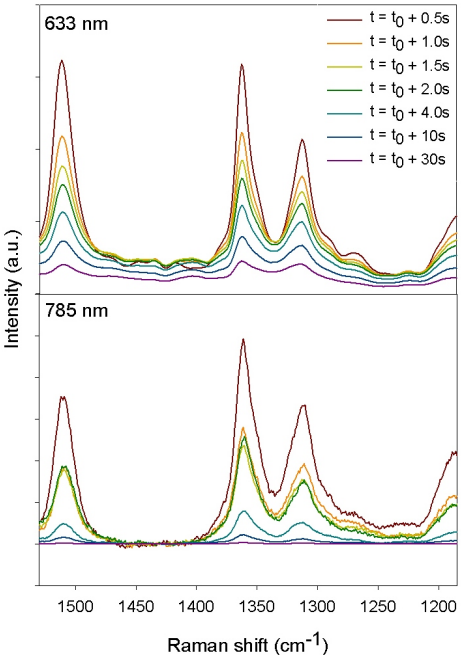

Figure S5: Comparison of the photo-degradation of Rh6G in air using a 785 nm laser (laser power 1 mW at sample) and a 633 nm laser (laser power 160 mW at sample) for Al_2O_3-supported Ag nanocubes.